Journal of Ceramic Processing Research. Vol. 21, No. 6, pp. 731~735 (2020)
(Received 30 July 2020, Received in revised form 2 September 2020, Accepted 2 October 2020)
https://doi.org/10.36410/jcpr.2020.21.6.731

J O U R N A L O F
Ceramic Processing Research

Enhanced the electrochemical performances of Ni-rich $LiNi_{0.8}Co_{0.1}Mn_{0.1}O_2$ cathode by ZrO_2 coating

Sung-Joo Jo[a,#], Hyun-Soo Kim[b,#], Do-Yeong Hwang[a], Bong-Soo Jin[b], Seong-Ju Sim[b], Jae-Soo Shin[a] and Seung-Hwan Lee[a,*]

[a]*Department of Advanced Materials Engineering, Daejeon University, Daejeon 34520, Republic of Korea*
[b]*Next-Generation Battery Research Center, Korea Electrotechnology Research Institute, Changwon, 641-120, South Korea*

ZrO_2 coated Ni-rich $LiNi_{0.8}Co_{0.1}Mn_{0.1}O_2$ cathode has enhanced electrochemical performance and stability compared with the pristine. The discharge capacity of both samples have no significant difference. However, the 1.77 wt% ZrO_2 coated $LiNi_{0.8}Co_{0.1}Mn_{0.1}O_2$ material delivers enhanced charge-discharge cycling (capacity retention of 97.1 % after 100 cycles at 0.5 C) while the capacity retention of pristine is 94.8 % under the same condition. Based on these, we can infer that the ZrO_2 coated $LiNi_{0.8}Co_{0.1}Mn_{0.1}O_2$ material shows great cyclability, originated from suppressing undesirable side reaction and decrease effectively electrolyte decomposition reaction. Therefore, the ZrO_2 coated Ni-rich $LiNi_{0.8}Co_{0.1}Mn_{0.1}O_2$ cathode can be considered as an effective strategy for long-life Li-ion batteries.

Keywords: ZrO_2, $LiNi_{0.8}Co_{0.1}Mn_{0.1}O_2$, electrochemical performances.

Introduction

Li-ion batteries (LIBs) have attracted a lot of attention for electric vehicles (EVs), mobile devices, plug-in hybrid electric vehicles (PHEVs), hybrid electric vehicles (HEVs) and residential energy storage applications. This is because LIBs have an advantage of high operating voltage and energy densities, power performance, low price, long lifetime and good stability compared to traditional batteries [1]. However, LIBs suffer from severe potential deposition and capacity fading when charge-discharge cycling. The energy density, lifetime, material cost and stability are essential criteria for assessing if they can be used in practical application in LIBs. Because the energy density of the LIBs is extremely dependent on the cathode material, thus, significant efforts have been conducted for high-performance cathode material [2].

In Particular, the layered nickel-rich oxide $LiNi_{1-x-y}Co_xMn_yO_2$ ($x > 0.8$, NCM) cathodes have drawn substantial interest [3]. Among various cathode materials, Nickel-rich NCM shows good electrochemical performance and it is considered as one of most effective cathode materials owing to low price and elevated electrochemical performances [4-5]. The superior energy density, excellent thermal stability and cyclability of Ni-rich NCM made it an ideal candidate for next-generation cathode material. However, high Ni content also results in irreversible capacity and poor cycling performance owing to the similar ionic radius of Ni^{2+} and Li^+ [6]. Especially, at higher temperature, the structural instability can lead to rapid performance fading of Ni-rich NCM [7]. To overcome these problems, various strategies such as TiO_2, SiO_2 and carbon coating and/or V, B and Mo doping [8-13] have been performed.

Among them, in this work, we synthesized well-crystallized ZrO_2 coated $LiNi_{0.8}Co_{0.1}Mn_{0.1}O_2$ (NCM811) in order to stabilize the structure and improve electrochemical performances. Consequently, the ZrO_2 coated NCM811 can be considered for advanced cathode material.

Experimental

Co-precipitation method was used to synthesize the Ni-rich NCM811 powders. the Ni-rich NCM811 powders were synthesized by using co-precipitation method $NiSO_4$-$6H_2O$, $CoSO_4$-$7H_2O$ and $MnSO_4$-H_2O were prepared to assemble $Ni_{0.8}Co_{0.1}Mn_{0.1}(OH)_2$ precursor. The chelating agent were comprised of NaOH and NH_4OH solution. The as-prepared spherical $Ni_{0.8}Co_{0.1}Mn_{0.1}(OH)_2$ precursor was used to mix with LiOH-H_2O at a molar ratio 1.05 : 1. After that, the mixture was fired at 480 °C for 5 h. Then the mixture was cooled down at 750 °C in air for 15 h. For surface coating, all samples of ZrO_2 coated Ni-rich NCM811 were synthesized exploiting different ratios of ZrO_2: Ni-rich NCM811 and then heated at 500 °C in air for 5 h.

[#]Sung-Joo Jo and Hyun-Soo Kim contributed equally.
*Corresponding author:
Tel : +82-42-280-2414
E-mail: shlee@dju.kr

The cathodes were prepared by mixing Ni-rich NCM811 powder, conductive carbon black binder and polyvinylidene fluoride in the weight ratio of 96 wt%: 2 wt%: 2 wt%. Afterwards, N-Methyl pyrrolidinone (NMP) solvent was included in the cathodes. The 2032 coin cells were compounded with Lithium metal disc in argon-gas-filled glove box as an anode. The electrolyte was consisted of 1 M $LiPF_6$ in ethylene carbonate, dimethyl carbonate, and ethyl methyl carbonate (EC:DMC:EMC 1:1:1 in volume). The polyethylene (PE, 20 μm) was used as a separator.

The XRD (Philips, X-pert PRO MPD) was used to measure the crystalline phase of samples. The FE-SEM (Hitachi S-4800) was prepared to observe the morphology of the pristine and ZrO_2 coated samples. The electron diffraction spectroscopy (EDS) was used in order to identify the component elements on the surface of particles. The electrochemical performances were measured with an equipment (TOSCAT-3100, Toyo system). The Electrochemical Impedance Spectroscopy (EIS) was measured with frequency range from 1 MHz to 100 mHz and the amplitude of the AC signal of 10 mV.

Results and Discussion

Fig. 1 shows the X-ray diffraction (XRD) spectra of the pristine and ZrO_2 coated NCM811. The shape of all samples is identical without secondary peaks since ZrO_2 coating do not affect the crystal structure of NCM811 materials. Overall, main diffraction peaks are indexed as a layered oxide structure in the hexagonal α-$NaFeO_2$ structure with a space group of R-3m [14]. Both obvious splitting of the (018)/(110) and (006)/(102) peaks suggests well-ordered layered structure. Also, the ratio of the intensities of (003) and (104) peaks (I(003)/I(104)) are regarded as index of cation mixing [15]. The cation ordering is resulted from the similar radius of Ni^{2+} (0.69 Å) and Li^+ (0.76 Å) at the 3a site [16]. The I(003)/I(104) of all samples are above 1.2, demonstrating superior cation ordering, which is regarded as an one of the important factor for good electrochemical performance.

Fig. 2 shows the FESEM images of (a-b) pristine and

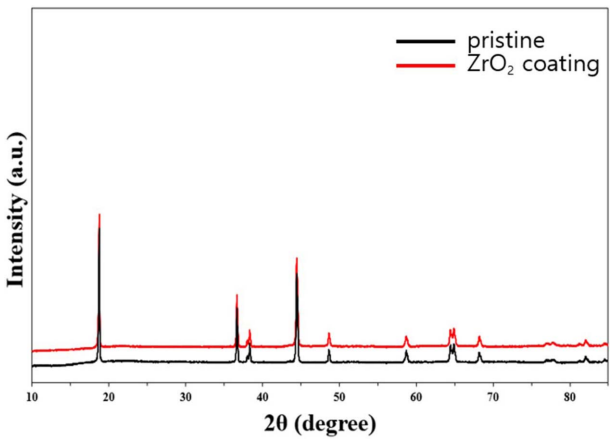

Fig. 1. XRD patterns of the pristine and ZrO_2 coated Ni-rich NCM811.

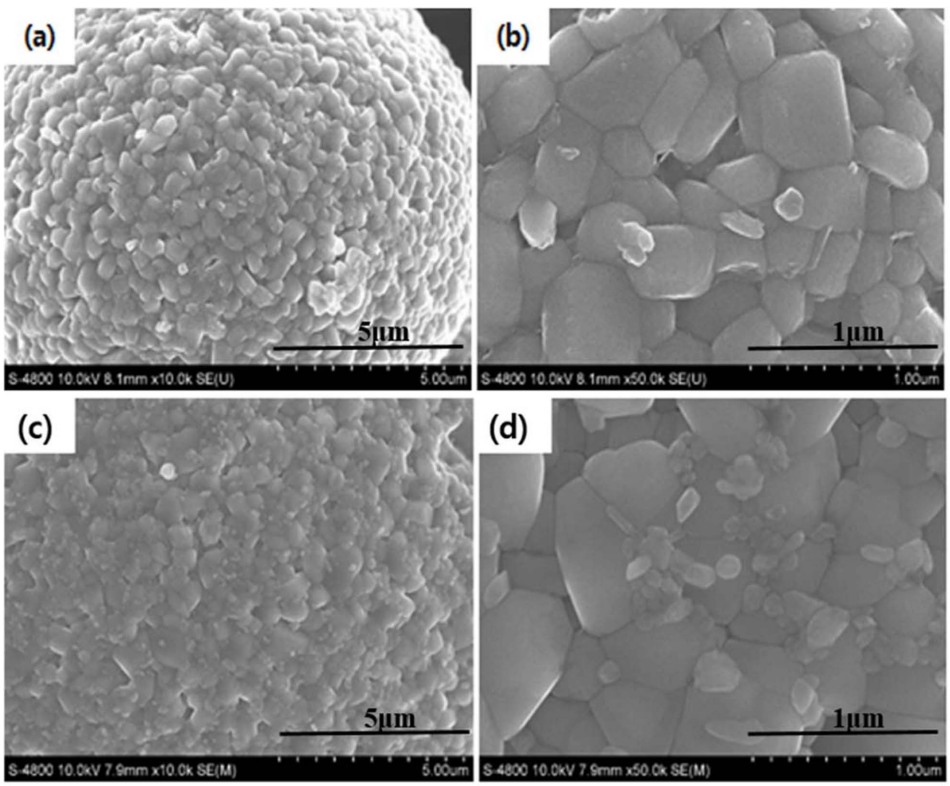

Fig. 2. FESEM images of the (a-b) pristine and (c-d) ZrO_2 coated Ni-rich NCM811.

(c-d) ZrO_2 coated NCM811 cathode materials. The pristine and ZrO_2 coated NCM811 sample have similar the morphology (particles size and shape) [17]. All samples have spherical morphology secondary particles with the average size of 15 ~ 20 μm, which is composed of numerous primary particles about 300 ~ 500 nm in diameter. The benefit of spherical secondary particle can achieve both high tap density and energy density. The surface of ZrO_2 coated NCM811 shows slightly rough as compared to pristine NCM811.

EDS (Energy Dispersive X-ray Spectroscopy) spectrum analysis of ZrO_2 coated NCM811 sample are conducted, as shown in Fig. 3. It can be confirmed that the Ni, Co, Mn and Zr are equally distributed and the amount of ZrO_2 is 1.77 wt%. The ZrO_2 coating can decrease the contact area between the cathode and the electrolyte, resulting in suppressing the electrolyte degradation while charge-discharge is cycling [18].

In order to investigate the long-term performance, Fig. 4 presents the cycle performance of the pristine and ZrO_2 coated NCM811 with vinylene carbonate (VC) and propane sultone (PS) additives. The cycle performances are measured at 0.5 C in the voltage between 3.0 and 4.3 V. It has been proved that additives can increase the cyclability for both samples since additive is designed to form the passivating layer on the surface, which can deactivate the active "catalytic" centers [19]. The ZrO_2 coated sample exhibits lower capacity fading than pristine sample after 100 charge-discharge cycles. This is because ZrO_2 coating could stabilize the interface between NCM811 and electrolyte. The ZrO_2 coated and pristine NCM811 have capacity retentions of 97.1% and 94.8%, respectively, after 100 cycles. We can confirm that the ZrO_2 coating effectively delay the capacity fading. In other words, it is demonstrated that the ZrO_2 coating on the Ni-rich NCM811 leads to superior cycle performance. This is because the bond dissociation energies of Zr-O, Ni-O, Co-O and Mn-O

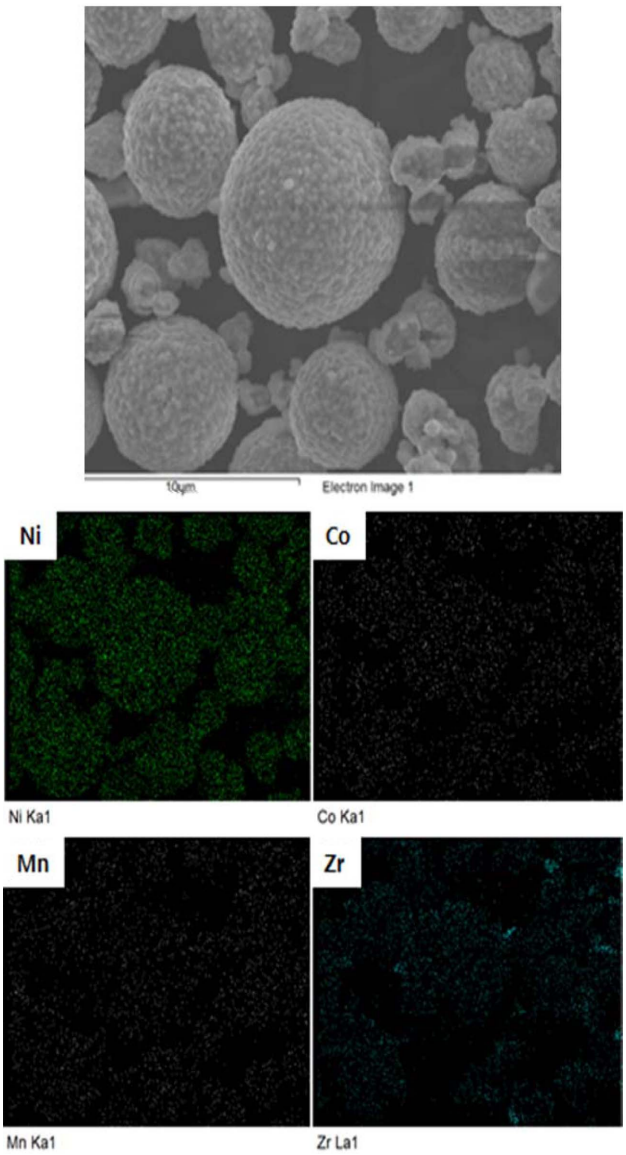

Fig. 3. EDS mapping of the ZrO_2 coated Ni-rich NCM811.

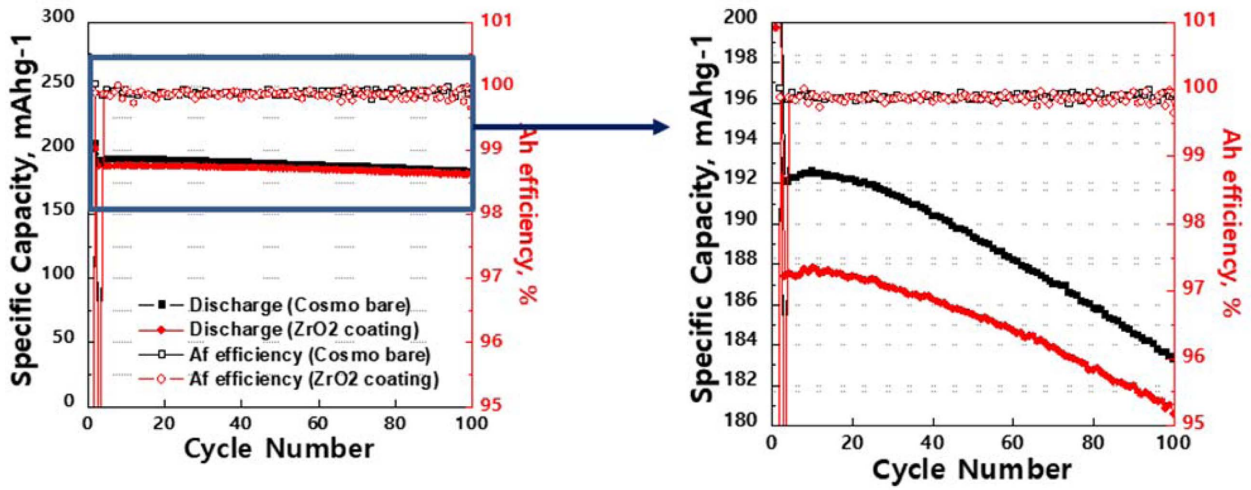

Fig. 4. Cycling performance of the pristine and ZrO_2 coated Ni-rich NCM811.

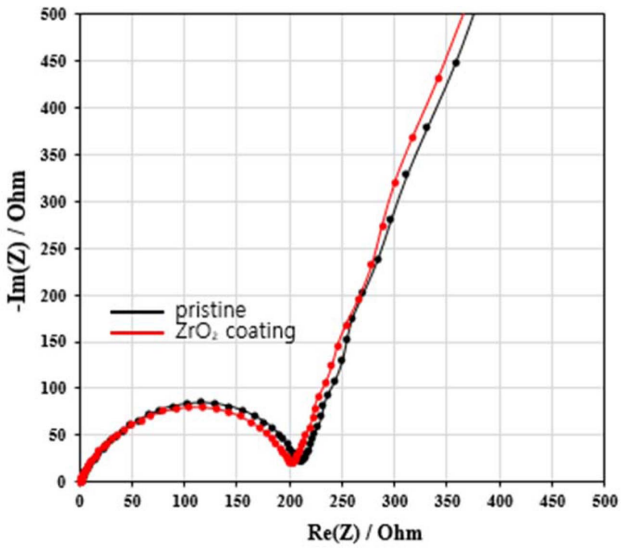

Fig. 5. Nyquist plots of the pristine and ZrO_2 coated Ni-rich NCM811.

Table 1. Value of R_e and R_{ct} of pristine and NCM811.

	R_e	R_{ct}
Pristine	1.12 Ω	211.5 Ω
ZrO_2 coated NCM811	1.08 Ω	203.7 Ω

have 760, 391.6, 368 and 402 kJ·mol^{-1} at 25 °C. The excellent cyclability of ZrO_2 coated Ni-rich NCM811 is closely related to the stable crystal structure, resulting from stronger iono-covalent of Zr-O [20].

Electrochemical Impedance Spectroscopy (EIS) measurements are used in order to investigate the charge-transfer kinetics of the electrodes. Nyquist plots of the pristine and the ZrO_2 coated NCM811 are measured after first cycle in the voltage range 3.0 – 4.3 V. Usually, Nyquist plot is composed of semicircle and one slope. Fig. 5 shows the EIS curves of the pristine and ZrO_2 coated NCM811. All samples have same electrolyte resistance (R_e) in the high-frequency because we used same electrolyte. The medium-frequency semicircle is contributed to the resistance of R_{ct} at the interface between the surface of the particles and the electrolyte [21]. The straight line of low frequency region is the Warburg impedance (W). There is a gap between pristine and ZrO_2 coated Ni-rich NCM811 for R_{ct}. The R_{ct} of ZrO_2 coated NCM811 is lower than the R_{ct} of pristine. After first cycle, the R_{ct} of pristine is 211.5 Ω, while the R_{ct} of ZrO_2 coated NCM811 is 203.7 Ω. This is because the ZrO_2 coating layer suppresses the formation of SEI due to accelerating the Li^+ movement at the surface of cathode [21]. Based on this, we can infer that ZrO_2 coating can reduce side reaction, cell impedance increases and R_{ct}. Therefore, the better cycle performance of ZrO_2 coating can be explained by lower R_{ct}.

Conclusions

In this work, we prepare the ZrO_2 coating on the surface of Ni-rich NCM811 cathode in order to enhance the electrochemical performance. The ZrO_2 coating has no effect on the crystal structure, particle size and shape. It is proved that ZrO_2 can not only stabilize the NCM811 structure but also improve the electrochemical performances due to the deceasing side reaction and the increasing electrochemical reaction kinetics of lithium ion. These factors can enable good cycling performance. Therefore, the ZrO_2 coating lead to being considered as an efficient way for Ni-rich NCM811 cathode.

Acknowledgement

This research was supported by the Daejeon University fund (2020)

References

1. W.S. Cho, S.M. Kim, K.W. Lee, J.H. Song, Y.N. Jo, T.E. Yim, H.T. Kim, J.S. Kim, and Y.J. Kim, Electrochim. Acta. 198 (2016) 77-83.
2. Q. Hou, G. Cao, P. Wang, D. Zhao, X. Cui, S. Li, and C. Li, J. Alloy. Comp. 747 (2018) 796-802.
3. J.Z. Kong, Y. Chen, Y.Q. Cao, Q.Z. Wang, A.D. Li, H. Li, and F. Zhou, J. Alloy. Comp. 799 (2019) 89-98.
4. A.Y. Kim, F. Strauss, T. Bartscch, J.H. Teo, T. Hatsukade, A. Mazilkin, J. Janek, P. Hartmann, and T. Brezesinski, Chem. Mater. 31 (2019) 9664-9672.
5. C.S. Yoon, H.H. Ryu, G.T. Park, J.H. Kim, K.H. Kim, and Y.K. Sun, J. Mater. Chem. A. 6 (2018) 4126.
6. S.J. Sim, S.H. Lee, B.S. Jin, and H.S. Kim, Sci. Rep. 9 (2019) 8952.
7. X. Li, K. Zhang, M. S. Wang, Y. Liu, M. Z. Qu, W. Zhao, and J. Zheng, Sustain. Energy Fuels. 2 (2018) 413-421.
8. Y.H. Cho, Y.S. Lee, S.A. Park, Y.I. Lee, and J.P. Cho, Electrochim. Acta 56.1 (2010) 333-339.
9. S.H. Lee, G.J. Park, S.J. Sim, B.S. Jin, and H.S. Kim, J. Alloy. Comp. 791 (2019) 193-199.
10. Q. Hou, G. Cao, P. Wang, D. Zhao, X. Cui, S. Li, and C. Li, J. Alloy. Comp. 747 (2018) 796-802.
11. S.J. Sim, S.H. Lee, B.S. Jin, and H.S. Kim, Sci. Rep. 9 (2019) 8952.
12. L. Pan, Y. Xia, B. Qiu, H. Zhao, H. Guo, K. Jia, Q. Gu, and Z. Liu, J. Power Sources. 327 (2016) 273-280.
13. Y. Li, Q. Su, Q. Han, P. Li, L. Li, C. Xu, X. Cao, and G. Cao, Ceram. Int. 43 (2017) 3483-3488.
14. G. Shang, Y. Tang, Y. Lai, J. Wu, X. Yang, H. Li, C. Peng, J. Zheng, and Z. Zhang, 423 (2019) 246-254.
15. J. Yang and Y. Xia, J. Electrochem. Soc. 163 (2016) 2665-2672.
16. J.Z. Kong, Y. Chen, Y.Q. Cao, Q.Z. Wang, A.D. Li, H. Li, and F. Zhou, J. Alloy. Comp. 799 (2019) 89-98.
17. F. Schipper, H. Bouzaglo, M. Dixit, E. M. Erickson, T. Weigle, M. Talianker, J. Grinblat, L. Burstein, M. Schmidt, J. Lampert, C. Erk, B. Markovsky, D.T. Major, and D. Aurbach, Adv. Energy Mater. 8.4 (2018) 1701682.
18. Z. Wang, E. Liu, L. Guo, C. Shi, C. He, J. Li, and N. Zhao, Surf. Coat. Technol. 235 (2013) 570-576.

19. Z.D. Li, Y.C. Zhang, H.F. Xiang, X.H. Ma, Q.F. Yuan, Q.S. Wang, and C.H. Chen, J. Power Sources. 240 (2013) 471-475.
20. S. Chang, Y. Chen, Y. Li, J. Guo, Q. Su, J. Zhu, G. Cao, and W. Li, J. Alloy. Comp. 781 (2019) 496-503.
21. J.W. Seok, J. Lee, T. Rodgers, D.H. Ko, D.H. Ko, and J.H. Shim, Trans. Electr. Electron. Mater. 20 (2019) 548-553.